

Differential HBT Applied to Relativistic Fluid Dynamics

L.P. Csernai¹, S. Velle¹, and D.J. Wang^{1,2}

¹ *Institute of Physics and Technology, University of Bergen, Allegaten 55, 5007 Bergen, Norway*

² *Key Laboratory of Quark and Lepton Physics (MOE) and Institute of Particle Physics, Central China Normal University, Wuhan 430079, China.*

(Dated: May 6, 2013)

The earlier introduced Differential HBT method aiming for detecting rotation is used to analyse the fluid dynamical model results of ultra-relativistic heavy ion reactions where the initial state has substantial angular momentum. The rotation effect and Kelvin Helmholtz Instability, lead to space-time momentum correlations, which can be detected by the method.

PACS numbers: 25.75.-q, 24.70.+s

Peripheral heavy ion collisions have high angular momentum, rapidly increasing with increasing beam energy. This is realized in rotating flow, large velocity shear, vorticity and circulation. Viscous, explosive expansion leads to the decrease of vorticity and circulation with time, however, with small viscosity the vorticity may remain significant at the final freeze-out (FO) stages. The earlier introduced Differential HBT method, a combination from standard two particle correlation functions, is adequate to analyze rotating systems. This was shown in few source models [1]. Now we look at this method and its results in a high resolution, Particle In Cell (PIC) fluid dynamics model. This model was used to predict the rotation in peripheral ultra-relativistic reactions [2], to point out the possibility of Kelvin Helmholtz Instability (KHI) [3], flow vorticity [4] and polarization [5]. The model was also tested for its numerical viscosity and the resulting entropy production [6].

One of the important observation in Ref. [1] is that in case of a globally symmetric fluid dynamical configuration the correlation function only includes $\cos(\alpha\mathbf{v})$ and $\cosh(\alpha\mathbf{v})$ terms, therefore it will not depend on the *direction* of the velocity, only on its magnitude. The *direction* dependence becomes apparent in the correlation function only if we take into account that due to the radial expansion and the opacity of the strongly interacting QGP, the emission probability from the far side of the system is reduced compared to the side of the system facing the detector.

Correlation Function from Fluid Dynamics: The pion correlation function is defined as the inclusive two-particle distribution divided by the product of the inclusive one-particle distributions, such that [7]:

$$C(p_1, p_2) = \frac{P_2(p_1, p_2)}{P_1(p_1)P_1(p_2)}, \quad (1)$$

where p_1 and p_2 are the 4-momenta of pions. We introduce the center-of-mass momentum ¹: $k = \frac{1}{2}(p_1 + p_2)$,

and the relative momentum $q = p_1 - p_2$, where from the mass-shell condition [7] $q^0 = \mathbf{k}\mathbf{q}/k^0$. We use a method for moving sources presented in Ref. [8].

$$C(k, q) = 1 + \frac{R(k, q)}{\left| \int d^4x S(x, k) \right|^2}, \quad (2)$$

where

$$R(k, q) = \int d^4x_1 d^4x_2 \cos[q(x_1 - x_2)] \times S(x_1, k + q/2) S(x_2, k - q/2). \quad (3)$$

Using the emission function $S(x, k)$, discussed in refs. [1], here $R(k, q)$ can be calculated [8] via the function

$$J(k, q) = \int d^4x S(x, k + q/2) \exp(iqx), \quad (4)$$

and we obtain the $R(k, q)$ function as $R(k, q) = \text{Re}[J(k, q) J(k, -q)]$.

We estimate the local pion density by the specific entropy, $\sigma(x)$, as $n_\pi(x) \propto n(x)\sigma(x)$, where $n(x)$ is the proper net baryon charge density. Thus the local invariant pion density is given by the Jüttner distribution as

$$f^J(x, p) = \frac{n(x)\sigma(x)}{C_\pi} \exp\left(-\frac{p^\mu u_\mu(x)}{T(x)}\right), \quad (5)$$

where $C_\pi = 4\pi m_\pi^2 T K_2(m_\pi/T)$, at temperature T , and K_2 is a modified Bessel function.

We assume that the single particle distributions, $f(x, p)$, in the source functions are Jüttner distributions, which depend on the local velocity, $u^\mu(x)$, and we use the notation $u_1 = u(x_1) = u^\mu(x_1)$.

If we assume that the two coincident particles originate from two points, x_1 and x_2 , the expression of the correlation function, Eq. (3) will be become [1]

$$R(k, q) = \int d^4x_1 d^4x_2 S(x_1, k) S(x_2, k) \cos[q(x_1 - x_2)] \times \exp\left[-\frac{q}{2} \cdot \left(\frac{u(x_1)}{T(x_1)} - \frac{u(x_2)}{T(x_2)}\right)\right], \quad (6)$$

and the corresponding $J(k, q)$ -function is

$$J(k, q) = \int d^4x S(x, k) \exp\left[-\frac{q \cdot u(x)}{2T(x)}\right] \exp(iqx), \quad (7)$$

¹ The vector \mathbf{k} is the wavenumber vector, $\mathbf{k} = \mathbf{p}/\hbar$ so for numerical calculations we have to use that $\hbar c = 197.327$ MeV fm., The same applies to \mathbf{q} .

In Ref. [1] different one, two and four source systems were tested with and without rotation. Here we study only the case where the emission is *asymmetric* and dominated by the fluid elements facing the detector.

In numerical fluid dynamical studies of symmetric (A+A) nuclear collision the initial state is symmetric around the center of mass (c.m.) of the system, and (if we do not consider random fluctuations) this symmetry is preserved during the fluid dynamical evolution.

Let us consider the usual conventions, z is the beam axis, and the positive z -direction is the direction of the projectile beam. The impact parameter vector points into the positive x -direction, i.e. towards the projectile. Finally the y -axis is orthogonal to both.

The fluid dynamical system, without fluctuations can be considered as a set of symmetric pairs of fluid cells.

The emission probabilities from the two fluid cells of a source pair are not equal.

If we have several fluid cell sources, s , with Gaussian space and time emission profiles, then the source function in Jüttner approximation is

$$\int d^4x S(x, k) = \sum_s \int d^3x_s dt_s S(x_s, k) = (2\pi R^2)^{3/2} \sum_s \frac{\gamma_s n_s(x) (k_\mu \hat{\sigma}_s^\mu)}{C_s} \exp\left[-\frac{k \cdot u_s}{T_s}\right], \quad (8)$$

where $n_s = n_\pi$, and the spatial integral over a cell volume is, $V_{cell} = (2\pi R^2)^{3/2}$ while the time integral is normalized to unity. Similarly the J -function is

$$J(k, q) = \sum_s e^{-\frac{q \cdot u_s}{2T_s}} e^{iqx_s} \int_S d^4x S_s(x, k) e^{iqx}. \quad (9)$$

We then assume that the freeze-out (FO) layer is relatively narrow compared to the spatial spread of the fluid cells, so that the peak emission times, t_s , of all fluid cells are the same. Then the $\exp(iq^0 t_s)$ factor drops out from the $J(k, q)J(k, -q)$ product.² This FO simplification is justified for rapid and simultaneous hadronization and FO from the plasma. For dilute and transparent matter the correlations from the time dependence of FO should be handled the same way as the spatial dependence.

Due to mirror symmetry with respect to the $[x, z]$, reaction plane, it is sufficient to describe the cells on the positive side of the y -axis. The other side is the mirror image of the positive side. Then we can evaluate the correlation function the same way as in Ref. [1].

Thus we define the quantities:

$$\begin{aligned} Q_c &= (2\pi R^2)^{3/2} \exp\left[-\frac{R^2 q^2}{2}\right], \\ P_s &= \frac{\gamma_s n_s}{C_s} \exp\left[-\frac{k_0 u_s^0}{T_s}\right], \\ Q_s^{(q)} &= \exp\left[-\frac{q_0 u_s^0}{2T_s}\right], \\ w_s &= (k_\mu \hat{\sigma}_s^\mu) \exp\left[-\frac{\Theta_s^2 q_0^2}{2}\right], \end{aligned} \quad (10)$$

where $u_s^0 = \gamma_s$, the local 4-direction normal of the mean particle emission from an ST point of the flow is $\hat{\sigma}_s^\mu$ (assumed to be time-like), R is the size (radius) of the fluid cells, and Θ_s is the path length of the time integral from the ST point of the source, s , while assuming a Gaussian emission time profile [1]. The weights, w_s arise directly from the Cooper-Frye formula [9].

We can reassign the summation for pairs, so that $s = \{i, j, k\}$ will correspond to a pair of cells: at $\{i, j, k\}$ and its reflected pair across the c.m. point at the same time at $\{i^*, j^*, k^*\}$. Then the function $S(k, q)$ becomes

$$\int d^4x S(x, k) = (2\pi R^2)^{3/2} \times \sum_s P_s \left[w_s \exp\left(\frac{\mathbf{k} \mathbf{u}_s}{T_s}\right) + w_s^* \exp\left(\frac{\mathbf{k} \mathbf{u}_s^*}{T_s}\right) \right], \quad (11)$$

while, the function $J(k, q)$ becomes

$$\begin{aligned} J(k, q) &= Q_c \sum_s P_s \left[Q_s^{(q)} w_s \exp\left[\left(\mathbf{k} + \frac{\mathbf{q}}{2}\right) \frac{\mathbf{u}_s}{T_s}\right] e^{i\mathbf{q} \mathbf{x}_s} \right. \\ &\quad \left. + Q_s^{(q)} w_s^* \exp\left[\left(\mathbf{k} + \frac{\mathbf{q}}{2}\right) \frac{\mathbf{u}_s^*}{T_s}\right] e^{i\mathbf{q} \mathbf{x}_s^*} \right] \end{aligned} \quad (12)$$

Only the mirror symmetry across the participant c.m. is assumed, which is always true for globally symmetric, A+A, heavy ion collisions in a non-fluctuating fluid dynamical model calculation. Then the correlation function can be evaluated using Eqs. (2-4).

Based on the few source model results the Differential HBT method was introduced by evaluating the difference of two correlation functions measured at two symmetric angles, forward and backward shifted in the reaction plane in the participant c.m. frame by the same angle, i.e. at $\eta = \pm \text{const.}$, so that

$$\Delta C(k, q) \equiv C(k_+, q_{out}) - C(k_-, q_{out}). \quad (13)$$

For the exactly $\pm x$ -symmetric spatial configurations (i.e. $k_{+x} = k_{-x}$ and $k_{+z} = -k_{-z}$), e.g. central collisions or spherical expansion, $\Delta C(k, q)$ would vanish! It would become finite if the rotation introduces an asymmetry.

The Freeze-out Weights: While the flow symmetries discussed above depend on the initial collision symmetries, the weights do not follow these. The ansatz

² If the emission is happening through a layer with time-like normal, but the peak is not at constant t_s , but rather at constant τ_s , then we can adapt the coordinate system accordingly, i.e. we can use the τ, η coordinates instead of t, z , see e.g. [9].

used in Ref. [1] leads the weights as given in Eq. (10). These weights depend on the local mean emission direction $\hat{\sigma}^\mu$, the flow velocity at the emission point and the opacity along the integrated path of the propagation of the emitted particle along this direction. The emission probability from different points of the space time is discussed in more detail in Ref. [1] based primarily on Refs. [10, 11]. These considerations may be more involved than the ansatz taken over from [9]. The determination of the FO surface normal or the mean emission direction from the ST freeze-out layer and the emission profile in this layer are the subjects of present theoretical research, see [12–15]. Here we do not discuss the effect of opacity along the path of the emission.

The detector configuration is given by the two particles reaching a given detector in the direction of \mathbf{k} . Thus the emission weights depend on the direction of the normal of the emission surface and of the emission, i.e. $\hat{\sigma}$ and \hat{k} . Furthermore, most monte-carlo cascade type of studies indicate [12, 13, 16], that the majority of particles freezes out in a layer along a constant proper time hyperbola, with a dominant flow 4-velocity, which is normal to this hyperbola: $\hat{\sigma}^\mu \approx u^\mu$. The origin of the hyperbola is at a ST point, which at low beam energies precedes the impact of the Lorentz contracted nuclei [12].

We assume in the actual numerical calculations that in the expression of the weight, Eq. (10), $Q_s(q)$ is the same for all surface layer elements: $Q_s^{(q)} = Q^{(q)}$ and $\Theta_s = \Theta$, so that $w_s = (k_\mu \hat{\sigma}_s^\mu) \exp(-\Theta^2 q_0^2/2)$, where $\hat{\sigma}_{s\mu} = (\sigma_s^0, \boldsymbol{\sigma}_s)$, so that $k_\mu \hat{\sigma}_s^\mu = k^0 \sigma_s^0 + \mathbf{k} \cdot \boldsymbol{\sigma}_s$. If emission path time-length, Θ , tends to zero, then the time modifying factor becomes unity. With the choice $\hat{\sigma}_\mu = u_\mu$, the time-like FO normal is $\hat{\sigma}_{s\mu} = (\gamma_s, \mathbf{u}_s)$. Then $(k_\mu \hat{\sigma}_s^\mu) = \gamma_s k_0 + \mathbf{k} \cdot \mathbf{u}_s$. So the weight becomes

$$w_s = (\gamma_s k_0 + \mathbf{k} \cdot \mathbf{u}_s) \exp(-\Theta^2 q_0^2/2). \quad (14)$$

This weight is explicitly different for the mirror image cell at $\mathbf{x}_s^* \rightarrow -\mathbf{x}_s$, where $\mathbf{u}_s^* \rightarrow -\mathbf{u}_s$ and then $w_s^* = (\gamma_s k_0 - \mathbf{k} \cdot \mathbf{u}_s) \exp(-\Theta^2 q_0^2/2)$.

The weight factors appear both in the nominator and denominator of the correlator, so its normalization is balanced. On the other hand the role of the different factors in the weight have an effect to determine which cells contribute more or less to the result. This is a fundamental problem of the FO process, and in real situations it can get further convoluted if the hadronization and FO coincide in a rapid expansion.

Results: The sensitivity of the standard correlation function on the fluid cell velocities decreases with decreasing distances among the cells. So, with a large number of densely places fluid cells where all fluid cells contribute equally to the correlation function, the sensitivity on the flow velocity becomes negligibly weak.

Thus, the emission probability from different ST regions of the system is essential in the evaluation. This emission asymmetry due to the local flow velocity occurs also when the FO surface or layer is isochronous or if it happens at constant proper time.

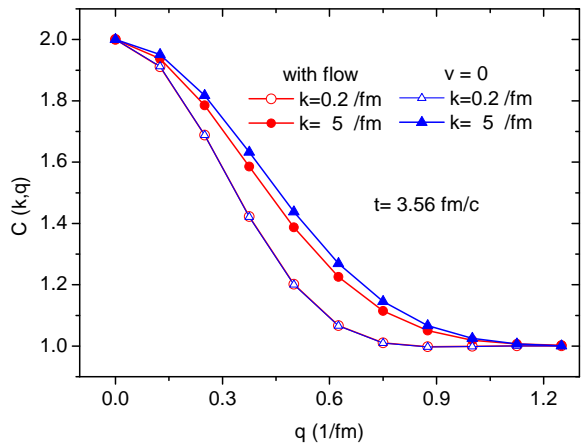


FIG. 1. (color online) The dependence of the standard correlation function in the \mathbf{k}_+ direction from the collective flow, at the final time.

We studied the fluid dynamical patterns of the calculations published in Ref. [3], where the appearance of the KHI is discussed under different conditions. We chose the configuration, where both the rotation [2], and **the KHI occurred**, at $b = 0.7b_{max}$ with high cell resolution and low numerical viscosity at LHC energies, where the angular momentum is large, $L \approx 10^6 \hbar$ [13].

We used the Differential HBT method introduced in Ref. [1] for simplified examples of a few fluid cells. These examples were spatially symmetric, thus the standard correlation function did not show any difference if it is measured at two symmetric \mathbf{k} and \mathbf{q} -out angles, e.g. in the reaction, [x-z] plane at $\mathbf{k}_+ = (k_x, 0, +k_z)$ $\mathbf{q}_+ = (q_x, 0, +q_z)$ and $\mathbf{k}_- = (k_x, 0, -k_z)$ $\mathbf{q}_- = (q_x, 0, -q_z)$, i.e. $\Delta C(k, q)$ vanished. Here we have chosen two directions at $\eta = \pm 0.76$, that is at polar angles of 90 ± 40 degrees. These are measurable with the ALICE TPC detector and at the ATLAS and CMS detectors also.

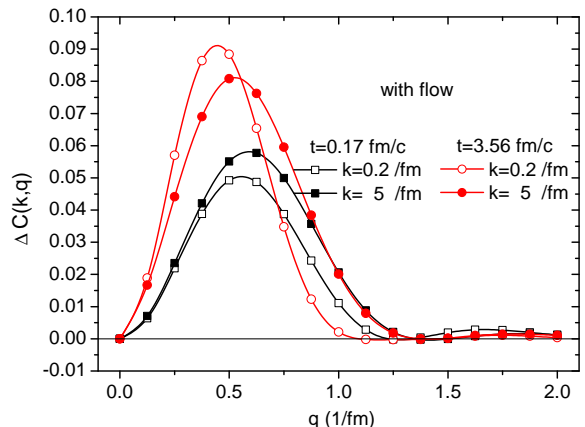


FIG. 2. (color online) The differential correlation function $\Delta C(k, q)$ at the initial and final times of flow development.

The standard correlation function is both influenced by the ST shape of the emitting source as well as its velocity distribution. The correlation function becomes

narrower in q with increasing time primarily due to the rapid expansion of the system. At the initial configuration the increase of $|\mathbf{k}|$ leads to a small increase of the width of the correlation function

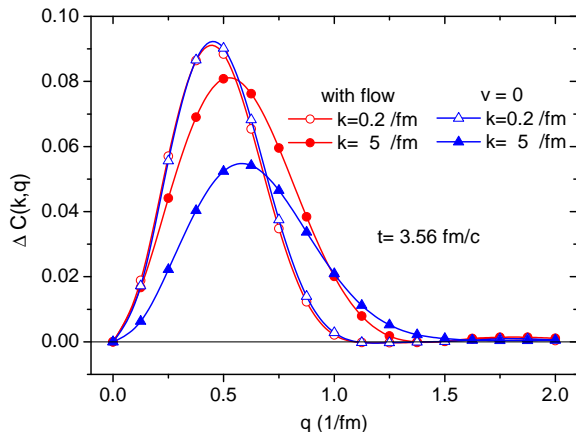


FIG. 3. (color online) The flow velocity dependence of the differential correlation function at the final time.

Nevertheless, in theoretical models we can switch off the flow, and analyse how the flow influences the correlation function and especially the differential correlation function, $\Delta C(k, q)$.

Fig. 1 compares the standard correlation functions with and without the collective flow at the final time moment. Here we see that the flow causes a decrease of the width in q for the distribution at high values of $|\mathbf{k}|$.

The differential correlation function is more sensitive on the flow as it is shown in the few source models. In Fig. 2 $\Delta C(k, q)$ is shown for the initial and final times. Although the amplitude of the differential correlation function is smaller the differences between the initial and

final configurations are significant. The dependence on $|\mathbf{k}|$ is especially large at the final time.

At the final time the flow dependence is again minimal at small momenta, $|\mathbf{k}|$, while at large momenta the flow leads to a change in the shape of the differential correlation function, and leads to an increase of its amplitude, Fig. 3. Here the expansion and the flow interfere with each other and this leads to a more complex behaviour. (The spatial configuration is not symmetric for $\pm x$, and this leads to nonvanishing $\Delta C(k, q)$ at $v = 0$ in Fig. 3.)

These tests demonstrate that the differential correlation function is sensitive to the flow and its rotation.

Conclusion: The present initial studies verify the dependence of the differential correlation function on the flow in general. At the same time it also shows that in realistic model situations the effect of the spatial size and shape, the flow expansion and the flow rotation all influence the differential correlation function. To entangle the three different effects from one another further more detailed model studies are necessary and a more detailed evaluation of the differential correlation function would be beneficial, e.g. in addition the present $q - out$ studies, the $q - side$ and $q - long$ components of the correlations functions should also be studied. Furthermore studies where \mathbf{k} points in the out of plane (y) direction may also be beneficial.

In addition theoretical model studies should be complemented with experimental investigations. In this case it is important to determine the precise Event by Event c.m. position of the participants [17], to be able to measure accurately the emission angles, which are crucial in the present $\Delta C(k, q)$ studies.

Acknowledgements: This work was supported in part by the Helmholtz International Center for FAIR. We thank F. Becattini, G. Graef, P. Huovinen and J. Manninen for comments.

-
- [1] L.P. Csernai, S. Velle, (2013) arXiv:1305.0385
 - [2] L.P. Csernai, V.K. Magas, H. Stöcker, and D.D. Strottman, Phys. Rev. C **84**, 024914 (2011).
 - [3] L.P. Csernai, D.D. Strottman and C. Anderlik, Phys. Rev. C **85**, 054901 (2012).
 - [4] L.P. Csernai, V.K. Magas, and D.J. Wang, Phys. Rev. C **87**, 034906 (2013).
 - [5] F. Becattini, L.P. Csernai, D.J. Wang, arXiv:1304.4427v1 [nucl-th]
 - [6] Sz. Horvát, V.K. Magas, D.D. Strottman, L.P. Csernai, Phys. Lett. B **692**, 277 (2010).
 - [7] W. Florkowski: *Phenomenology of Ultra-relativistic heavy-Ion Collisions*, World Scientific Publishing Co., Singapore (2010).
 - [8] A.N. Makhlin, Yu.M. Sinyukov, Z. Phys. C **39**, 69 (1988); S.V. Akkelin, Yu.M. Sinyukov, Z. Phys. C **72**, 501 (1996).
 - [9] T. Csörgő, Heavy Ion Phys. **15**, 1-80, (2002); arXiv:hep-ph/0001233v3
 - [10] E. Molnár, L. P. Csernai, V. K. Magas, Zs. I. Lazar, A. Nyiri, and K. Tamosiunas, J. Phys. G **34**, 1901 (2007).
 - [11] E. Molnár, L. P. Csernai, V. K. Magas, A. Nyiri, and K. Tamosiunas, Phys. Rev. C **74**, 024907 (2006).
 - [12] D. Anchishkin, V. Vovchenko, and L.P. Csernai, Phys. Rev. C **87**, 014906 (2013).
 - [13] V. Vovchenko, D. Anchishkin, and L.P. Csernai, in preparation.
 - [14] Y. Cheng, L.P. Csernai, V.K. Magas, B.R. Schlei, and D. Strottman, Phys. Rev. C **81**, 064910 (2010).
 - [15] P. Huovinen, H. Petersen, Eur. Phys. J. A **48**, 171 (2012)
 - [16] D. Anchishkin, V. Vovchenko, and S. Yezhov, Eur. Phys. J. A, in press.
 - [17] L.P. Csernai, G. Eyyubova, V.K. Magas, Phys. Rev. C **86**, 024912 (2012).